ADVANCED HEALTHCARE MATERIALS
www.advhealthmat.c

Magnetic Nanoparticles-Embedded Enzyme-Inorganic Hybrid Nanoflowers with Enhanced Peroxidase-Like Activity and Substrate Channeling for Glucose Biosensing

Hong Jae Cheon, Manab Deb Adhikari, Minsoo Chung, Tai Duc Tran, Jungbae Kim, and Moon Il Kim**

It is reported that glucose oxidase (GOx)-copper hybrid nanoflowers embedded with Fe_3O_4 magnetic nanoparticles (MNPs) exhibit superior peroxidase-mimicking activity as well as substrate channeling for glucose detection. This is due to the synergistic integration of GOx, crystalline copper phosphates and MNPs being in close proximity within the nanoflowers. The preparation of MNP-embedded GOx-copper hybrid nanoflowers (MNPs-GOx NFs) begins with the facile conjugation of amine-functionalized MNPs with GOx molecules via electrostatic attraction, followed by the addition of copper sulfate that leads to full blooming of the hybrid nanoflowers. In the presence of glucose, the catalytic action of GOx entrapped in the nanoflowers generates H_2O_2, which is subsequently used by peroxidase-mimicking MNPs and copper phosphate crystals, located close to GOx molecules, to convert Amplex UltraRed substrate into a highly fluorescent product. Using this strategy, the target glucose is successfully determined with excellent selectivity, stability, and magnetic reusability. This biosensor based on hybrid nanoflowers also exhibits a high degree of precision and reproducibility when applied to real human blood samples. Such novel MNP-embedded enzyme-inorganic hybrid nanoflowers have a great potential to be expanded to any oxidases, which will be highly beneficial for the detection of various other clinically important target molecules.

1. Introduction

Currently, ≈200 million people worldwide are afflicted with diabetes mellitus, which is considered as one of the principal causes of death and disability as well as highly responsible for heart disease, kidney failure, and blindness.[1] To avoid diabetic emergencies, frequent testing of physiological blood glucose level is crucial for the confirmation of effective treatment. In this regard, the glucose detection techniques have been extensively studied in healthcare field.[2] Among diverse glucose detection strategies, the glucose biosensors employing GOx play a leading role due to their simplicity to perform with high selectivity and sensitivity. However, there are still unresolved issues of enzyme-based glucose determination, such as enzyme immobilization, limited operating condition, and instability. Therefore, the development of highly efficient glucose biosensors to enable convenient, stable, and accurate glucose level monitoring is still imperatively needed.[3]

Organic–inorganic hybrid nanostructures with flower-like morphology, termed nanoflowers, have received an increasing attention owing to their capability to greatly enhance the activity, stability, and durability of entrapped organic biomolecules.[4,5] Biomolecules, such as proteins or DNAs containing nitrogen atoms in their amide or amine groups, were suggested to form complexes with inorganic metal ions such as copper, zinc, cobalt, and manganese via coordination interactions, which drive nucleation of primary metal phosphate crystals and concomitant anisotropic growth to form highly branched, multilayered flower-like structures.[6,7] The synthetic procedure of nanoflowers is very simple by just coincubating biomolecules and metal ions in an aqueous phosphate buffer at around neutral pH and room temperature but yields a hierarchical structure with a large surface-to-volume ratio, which entraps a large amount of biomolecules without placing severe mass transfer limitations. Synthesis begins with the spontaneous formation of nanostructured biomolecule-metal phosphate complexes and generally takes 3 d for the flowers to bloom fully.[6] In our previous study, we have reported an innovative strategy to significantly reduce the time taken to synthesize nanoflowers from the conventional 3 d to only 5 min via sonication treatment, which greatly facilitates their practical utilization.[8] Based on these advantageous characteristics,

H. J. Cheon, M. Chung, T. D. Tran, Prof. M. I. Kim
Department of BioNano Technology
Gachon University
Gyeonggi 13120, South Korea
E-mail: moonil@gachon.ac.kr
Dr. M. D. Adhikari, Prof. J. Kim
Department of Chemical and Biological Engineering
Korea University
Seoul 02841, South Korea
E-mail: jbkim3@korea.ac.kr
The ORCID identification number(s) for the author(s) of this article can be found under https://doi.org/10.1002/adhm.201801507.

DOI: 10.1002/adhm.201801507

nanoflowers have been utilized in various areas including biosensors,[9,10] biocatalysts for protein digestion and dye removal,[11,12] and biofuel cells.[13]

Recently, several groups reported a strategy to incorporate multiple enzyme components within hybrid nanoflowers to detect target analytes from multistep cascade reactions.[14–16] Representatively, glucose oxidase (GOx) and horseradish peroxidase (HRP) were employed as two different enzyme components with copper sulfate in phosphate buffered saline (PBS), resulting in multienzyme incorporated hybrid nanoflowers, which can be utilized for detecting target glucose via the GOx-HRP mediated cascade enzyme reaction.[16] Furthermore, another type of organic components, such as antibody,[17] streptavidin,[18] or concanavalin A,[19] all of which have high affinity for their corresponding target molecules, were added to generally used enzymes and inorganic metal ions, to develop triple component-incorporated hybrid nanoflowers. The nanoflowers described above were proven to have multifunctionalities composed of biorecognition and signal amplification, which were arisen from the entrapped biomolecules, including antibody, streptavidin or concanavalin A, mediating specific recognition and the enzymes catalyzing signaling, respectively. The multifunctionality of nanoflowers allowed for the selective and sensitive detection of disease-indicating biomarkers or pathogenic bacteria in food.[18,20] These recent examples demonstrated the potential of nanoflowers with multiple-components to extend and diversify their applicability. However, there has been little effort to incorporate multiple inorganic components rather than biomolecular components within hybrid nanoflowers, presumably due to their intrinsic deficiency of amine or amide moieties, which are generally required as the starting sites to bloom the flower-like structures. Therefore, successful incorporation of inorganic components such as nanoparticles can make it possible to develop much more versatile nanoflowers due to their exceptionally unique characteristics including optical, catalytic, electronic, and magnetic properties.[21,22]

In the present study, we report a new class of multifunctional organic–inorganic hybrid nanoflowers that incorporate Fe_3O_4 magnetic nanoparticles (MNPs) within GOx-copper hybrid nanoflowers (MNPs-GOx NFs). MNPs have been utilized in many different applications, such as magnetic resonance imaging,[23] drug delivery,[24] and magnetic separation for repeated catalysis.[25] Recently, MNPs were reported as peroxidase mimics that may have diverse biotechnological applications.[26] However, there has been no study to successfully incorporate MNPs within hybrid nanoflowers until now. In this study, we confirmed that MNPs-GOx NFs exhibited superior peroxidase-like activity and allowed substrate channeling, both of which facilitated the cascade reaction mediated by GOx and peroxidase-mimicking MNPs and copper phosphate crystals, located in close proximity within hybrid nanoflowers, for the successful detection of target glucose. Various analytical characteristics of MNPs-GOx NFs and glucose sensing system based on them, such as specificity, sensitivity, stability, magnetic reusability, and detection precision were investigated.

2. Results and Discussion

Overall scheme for the synthesis of MNPs-GOx NFs and the detection mechanism for glucose sensing are illustrated in **Figure 1**. To efficiently incorporate MNPs with GOx within nanoflowers, MNPs were first functionalized with 3-aminopropyl triethoxysilane to prepare amine-functionalized MNPs, followed by 2 h incubation in a buffer solution adjusted at pH 5.5 with GOx molecules to induce electrostatic attraction between GOx

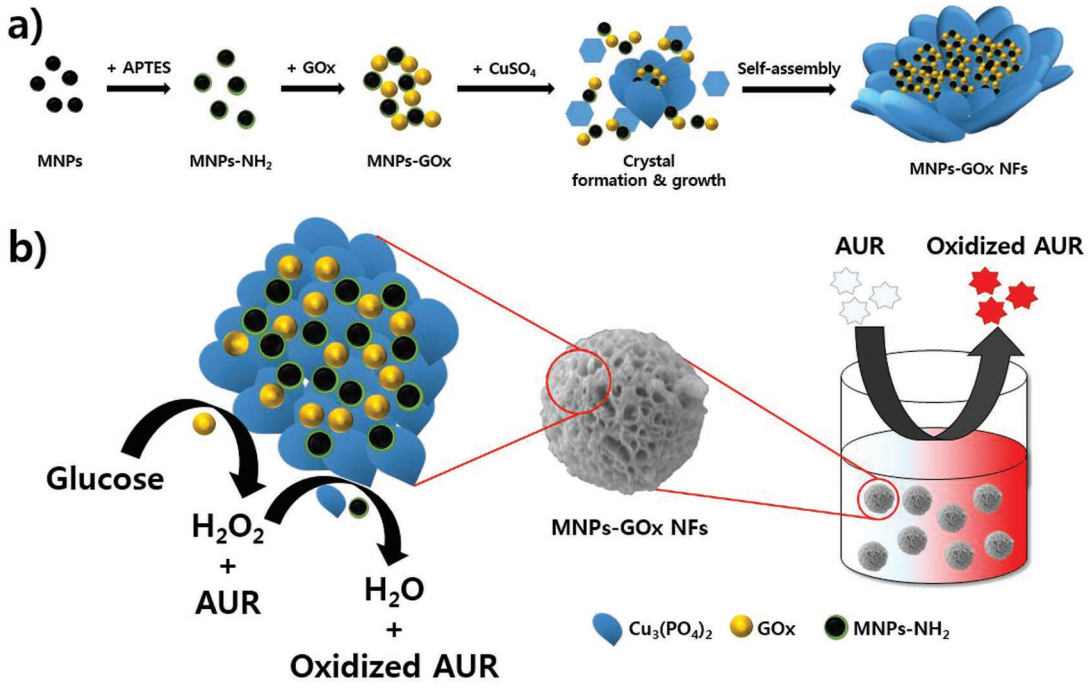

Figure 1. Schematic illustration for a) preparation of MNPs-GOx NFs and b) glucose detection mechanism via cascade reactions.

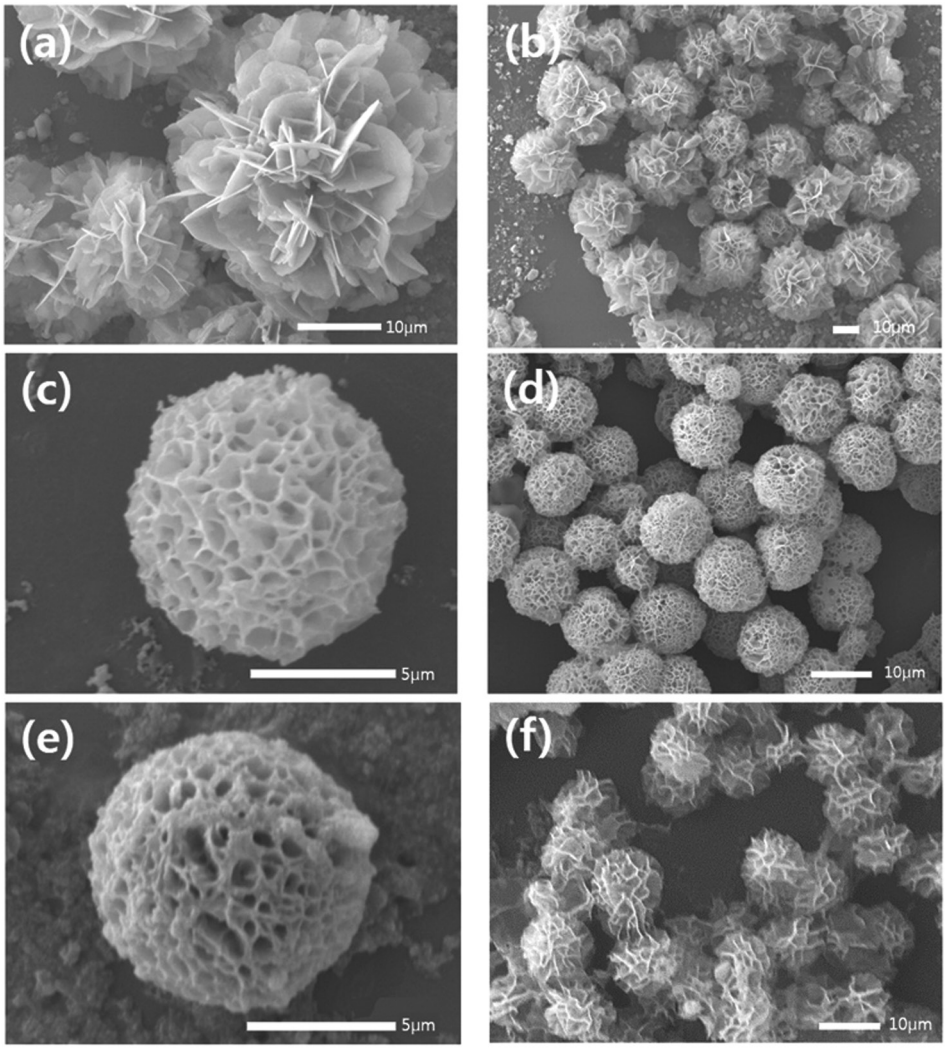

Figure 2. SEM images of a,b) MNPs NFs, c,d) GOx NFs, and e,f) MNPs-GOx NFs.

and amine-functionalized MNPs. Buffer solution containing copper (II) sulfate was added, and incubation at room temperature (RT) for 3 d induced full blooming of nanoflowers via the anisotropic growth of copper phosphate crystals. The amine or amide moieties preserved on the surface of GOx as well as MNPs are expected to form complexes with the applied copper ions mainly through the coordination interaction, which consequently mediates the formation of highly branched flower-like structures.[27] As expected, we were unable to observe flower-like structures when free MNPs rather than amine-functionalized MNPs were used for the synthesis of MNP-GOx NFs (Figure S1, Supporting Information). It was anticipated that MNPs-GOx NFs would serve as an efficient glucose biosensor due to the synergistic integration of MNPs, GOx, and crystalline copper phosphates in close proximity within the nanoflowers. Specifically, in the presence of target glucose, GOx entrapped in the nanoflowers catalyzes the oxidation of glucose to generate H_2O_2, which can be further used by the peroxidase-mimicking MNPs and copper phosphate crystals,[28,29] located close to GOx molecules, to convert the selected Amplex UltraRed (AUR) substrate into a highly fluorescent product (Figure 1).

The scanning electron microscopy (SEM) images of MNPs-copper hybrid nanoflowers (MNPs NFs), GOx-copper hybrid nanoflowers (GOx NFs), and MNPs-GOx NFs show flower-like hierarchical structures with a high surface-to-volume ratio in all cases (**Figure 2**). It was also observed that MNPs NFs showed much sharper and flatter petals of a larger size (≈30 μm in diameter) than GOx NFs, presumably due to the insufficient amount of active amine moieties on the surface of MNPs (≈10 nm) while GOx molecules (5.2 nm × 6.0 nm × 7.7 nm; ≈6.0 nm)[30] naturally possessing abundant amine and amide moieties, well distributed in their peptide backbones.[27] Much lower particular concentrations of MNPs (≈70×10^{-9} M) than that of GOx (≈1250×10^{-9} M) would also contribute to the reduced number of active amine moieties available for the synthesis of MNPs NFs. This presumably reveals that a decrease in the number of nucleation sites in MNPs results in nanoflowers of a bigger size with less-numbered and larger sized petals.[10] Both MNPs NFs and GOx NFs were incubated in PBS (pH 7.4) to bloom flowers similar to those from the conventional synthetic strategy.[6] However, a different buffer adjusted at pH 5.5 was employed to prepare MNPs-GOx NFs, in order to maintain

electrostatic attraction between MNPs and GOx, which was confirmed by zeta potential analysis (Figure S2, Supporting Information). Although complexation between copper ions and amine moieties was known to be less efficient in acidic pH than in neutral pH,[27] MNPs-GOx NFs were successfully prepared at a slightly acidic condition of pH 5.5, showing both similar size and morphology compared to those of GOx NFs.

We also confirmed that MNPs-GOx NFs were not correctly formed at pH 3 and pH 7.4 (Figure S3, Supporting Information), indicating the importance of synthetic buffer pH for the successful preparation of MNPs-GOx NFs. Considering the pI values of GOx (≈4.2)[31] and amine-functionalized MNPs (≈10.0),[32] it is presumed that no flower-like structure was produced at pH 3 due to the net positive surface charge of both MNPs and GOx, resulting in strong repulsion between MNPs and GOx, which does not provide good nucleation sites for the formation of nanoflowers (Figure S3a, Supporting Information). On the other hand, poorly grown petal-like morphologies at pH 7.4 (Figure S3c, Supporting Information) can be explained by stronger coordination bonding, which depletes most of the Cu^{2+} ions in the form of copper phosphate and interrupts the growth of hierarchical flower-like structures. In other words, optimized charge interaction between oppositely charged MNPs and GOx as well as efficient coordination interaction between Cu^{2+} and amine moieties of MNPs and GOx at pH 5.5 is critical for the successful preparation of MNP-GOx NFs. For the MNPs-GOx NFs, the utilization of 0.1 mg mL^{-1} of GOx with 1 mg mL^{-1} of MNPs achieved the highest encapsulation yield (over 90%), defined as the ratio of the amount of incorporated GOx to the total amount of GOx used (Table S1, Supporting Information), and this sample was used for further experiments.

To gain insights into the structures of MNPs-GOx NFs, they were subjected to X-ray diffraction (XRD), Fourier transform infrared (FT-IR) spectroscopy, transmission electron microscopy with energy dispersive X-ray spectroscopy, vibrating sample magnetometer (VSM), and Brunauer–Emmett–Teller (BET) analyses. The peaks in the XRD of MNPs NFs as well as MNPs-GOx NFs were found to match those in standard crystal structures of $Cu_3(PO_4)_2 \cdot 3H_2O$ (Joint Committee on Powder Diffraction Standards (JCPDS) 00-022-0548) and Fe_3O_4 (JCPDS 00-019-0629), indicating that crystalline copper phosphates as well as MNPs were incorporated in the nanoflowers (Figure S4a, Supporting Information). GOx NFs only showed peaks corresponding to $Cu_3(PO_4)_2 \cdot 3H_2O$ since GOx NFs did not incorporate any MNPs. In addition, the chemical structures of MNPs-GOx NFs were compared with those of MNPs NFs and GOx NFs using FT-IR (Figure S4b, Supporting Information). The peaks observed at 983–1042 cm^{-1} in the spectrums of all applied nanoflowers were attributed to P–O vibrations, clearly indicating the presence of phosphate groups in the nanoflowers.[33] Two characteristic peaks at 1625 and 1540 cm^{-1} for GOx NFs and 1630 and 1535 cm^{-1} for MNPs-GOx NFs were attributed to peptide bonds,[34] indicating that GOx molecules were encapsulated in both nanoflowers. The above absorption peaks were not observed from MNPs NFs due to the absence of protein molecules. The absorption peaks at about 3300–3340 and 530–540 cm^{-1}, observed for both MNPs NFs and MNPs-GOx NFs, were typical characteristics of the Fe—O bond and their hydroxyl groups,[35] confirming the presence of MNPs in both nanoflowers. As expected, the above two peaks were not observed for GOx NFs since they did not incorporate any MNPs. Elemental mappings of MNPs-GOx NFs from their scanning transmission electron microscopy (STEM) image provide direct proof for the formation of respective multicomponent incorporated nanoflowers, where representative elements corresponding to copper phosphate (Cu and P), MNPs (Fe), and GOx (N) were clearly observed throughout the nanoflowers (**Figure 3**a). MNPs corresponding to Fe elements were not evenly distributed and were aggregated in some regions on the outside of the flowers. This is presumably due to the fact that excess amount of MNPs may have high free energies and mobilities leading to some degree of aggregation caused by weak ferromagnetic interactions generated by dipole–dipole interactions.[36,37] However, there were still many MNPs homogeneously dispersed within the nanoflowers, possibly leading to enhanced peroxidase activity as compared to free MNPs, which are prone to aggregation when suspended in aqueous solution.[38,39] VSM analysis clearly indicated that both MNPs NFs and MNPs-GOx NFs have magnetic properties due to their incorporation of MNPs, whereas GOx NFs did not develop magnetic properties due to the absence of MNPs (Figure 3b). With large saturation magnetization, our target MNPs-GOx NFs could be separated from the reaction medium rapidly (within 30 s) and easily in an external magnetic field, which facilitates their recycling and reutilization (Figure 3c). The surface area, pore volume, and average pore diameter of MNPs-GOx NFs were determined to be 18.5 $m^2\ g^{-1}$, 0.094 $cm^3\ g^{-1}$, and 19.0 nm, respectively, using the BET method, confirming their porous structure as well as high surface-to-volume ratio (Figure S5, Supporting Information). All these characterizations confirm that MNPs-GOx NFs were successfully formed by incorporating MNPs, GOx, and crystalline copper phosphate within the nanoflowers.

Peroxidase-like activity of MNPs-GOx NFs was first examined by performing typical reactions using AUR as a substrate in the presence of H_2O_2. The results clearly showed that MNPs-GOx NFs display peroxidase activity by promoting the oxidation of AUR to produce specific fluorescence responses (**Figure 4**a), which can be explained by peroxidase-mimicking components of MNPs and copper phosphate crystals within the nanoflowers.[28] We then compared the peroxidase activity of MNPs-GOx NFs with those of MNPs NFs and GOx NFs. MNPs-GOx NFs as well as MNPs NFs enhanced peroxidase activity by displaying a fluorescence intensity approximately twofold higher than that of GOx NFs (Figure 4b), which may result from the enhancement of peroxidase activity by MNPs within the nanoflowers. Peroxidase activity of MNPs-GOx NFs varied depending on reaction environments including pH and temperature, and optimal activity was observed in weak basic conditions above 37 °C (Figure S6, Supporting Information). Based on these results, we adopted pH 7.0 and 37 °C as standard reaction conditions for further studies. Under the optimized conditions, the lowest concentration of H_2O_2 detectable using MNPs-GOx NFs based system was determined. Based on the data derived from a typical dose-response curve, as low as 10×10^{-6} M H_2O_2 can be detected within a linear range from 0.03×10^{-3} to 1×10^{-3} M, confirming that MNPs-GOx NFs could serve as a new nanohybrid, useful for the efficient identification of H_2O_2 (Figure 4c,d).

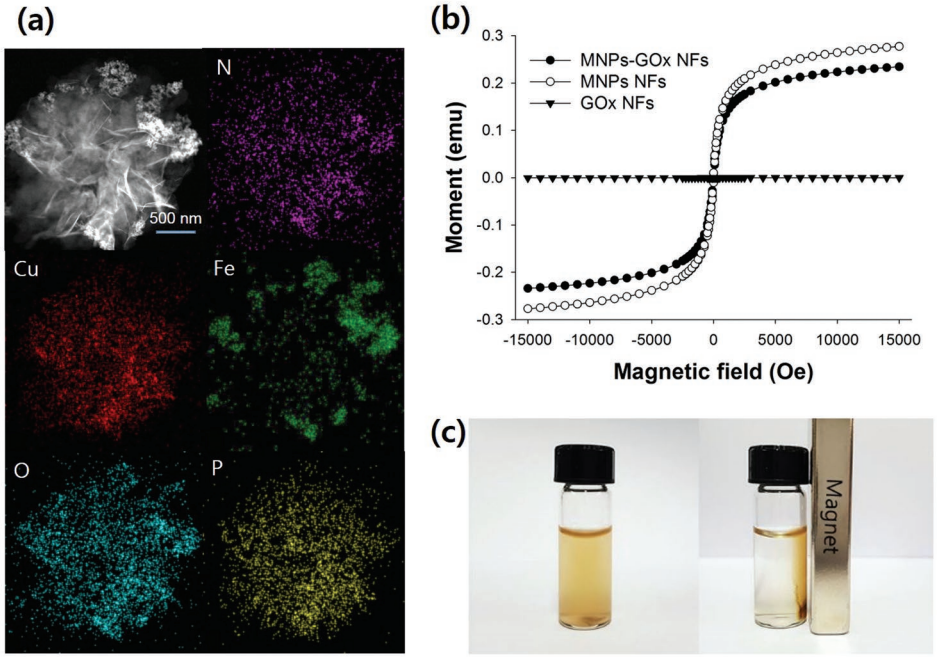

Figure 3. a) STEM image and elemental mappings of MNPs-GOx NFs. b) Magnetic properties of MNPs-GOx NFs, MNPs NFs, and GOx NFs. c) Pictures showing the facile magnetic separation for MNPs-GOx NFs.

The peroxidase activities of MNPs and copper phosphate crystals would be valuable for developing a glucose sensing system based on MNPs-GOx NFs. GOx entrapped within the nanoflowers catalyzes the oxidation of glucose to generate H_2O_2, which is used by both MNPs and copper phosphate crystals located near the GOx molecules, for enhanced conversion

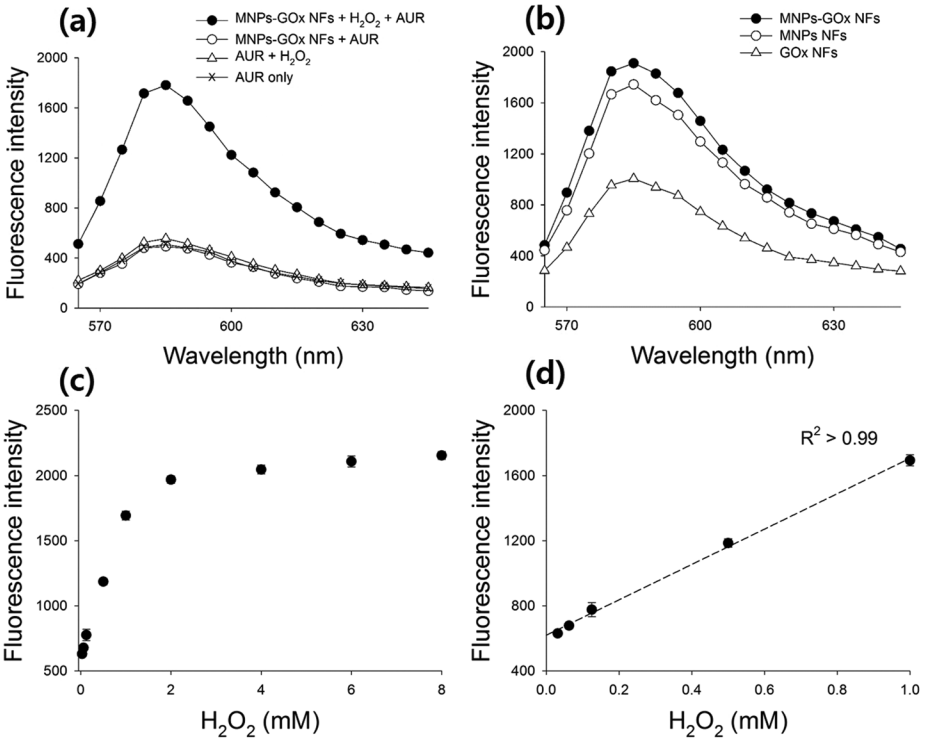

Figure 4. a) Fluorescence spectra of MNPs-GOx NFs induced AUR oxidation in the presence of H_2O_2. b) Comparison of peroxidase activities among MNPs-GOx NFs, MNPs NFs, and GOx NFs. c) Dose-response curves for H_2O_2 detection by MNPs-GOx NFs and d) corresponding linear calibration plots. Error bars represent standard deviations obtained from three independent measurements.

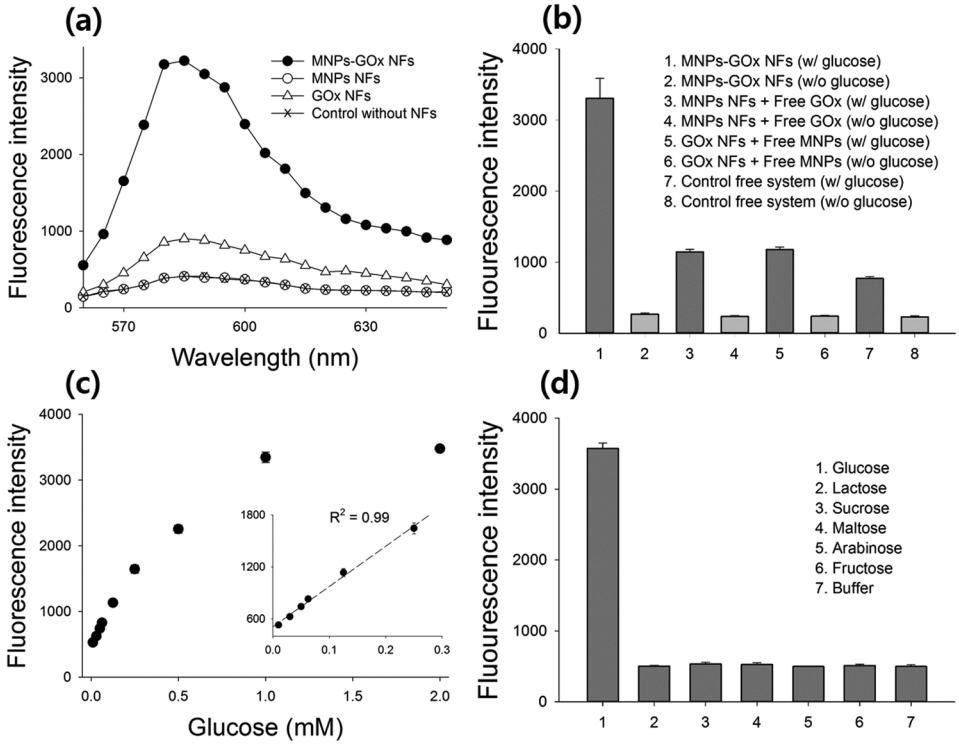

Figure 5. a) Fluorescence spectra for the comparison of glucose sensing activities among MNPs-GOx NFs, MNPs NFs, GOx NFs, and control without NFs (only glucose and AUR). b) Fluorescence intensities from AUR oxidation promoted by MNPs-GOx NFs (1 and 2), MNPs NFs with free GOx (3 and 4), GOx NFs with free MNPs (5 and 6), and control free system composed of free MNPs, free GOx, and BSA NFs (7 and 8). c) Dose-response curve and linear calibration plot of MNP-GOx-NFs for glucose detection. d) Selectivity of MNP-GOx-NFs toward target glucose. In selectivity assessment, glucose was used at 0.1×10^{-3} M while other sugars were used at 1×10^{-3} M. Error bars represent standard deviations obtained from three independent measurements.

of the AUR substrate into a highly fluorescent product. Through the typical reaction, target glucose was successfully detected by the generation of the respective fluorescence intensity (**Figure 5**a). As expected, no significant fluorescence signal was observed when we employed MNPs NFs due to the absence of GOx. GOx NFs also enabled the detection of glucose, although the resulting fluorescence intensity corresponding to target glucose was ≈3.5-fold lower than that of MNPs-GOx NFs. This result clearly indicated that sensing performance for target glucose was greatly enhanced by the incorporation of MNPs in GOx NFs.

We propose that spatial proximity of GOx, MNPs, and copper phosphate crystals present in MNPs-GOx NFs may facilitate the cascade enzyme reaction for target glucose detection through substrate channeling.[40] To gain an evidence to support this hypothesis, glucose sensing activity of MNPs-GOx NFs was evaluated and compared with those from control systems where either GOx or MNPs are incorporated within the nanoflowers and the other free component is simply mixed. We also evaluated the activity of nonintegrated systems where both GOx and MNPs were not integrated but simply mixed with bovine serum albumin (BSA)-copper hybrid nanoflowers (BSA NFs). The results showed that MNPs-GOx NFs exhibited a significantly enhanced glucose sensing activity, which is approximately threefold higher than that of the control systems composed of MNPs NFs or GOx NFs with their free counterparts, and approximately fourfold higher than that of the nonintegrated systems (Figure 5b). These results indicated that incorporation of both MNPs and GOx, located close together within the nanoflowers, was essential to achieve high catalytic performance of the cascade reaction for glucose detection. In particular, considering that MNPs NFs exhibit high peroxidase activity similar to MNPs-GOx NFs, it is noteworthy that MNPs-GOx NFs exhibit much higher activity for glucose detection than MNPs NFs mixed with free GOx. This can be explained by the spatial proximity of GOx with peroxidase-mimicking MNPs and copper phosphate crystals within the nanoflower matrices. The close distance among them enables H_2O_2 molecules, the product of GOx-catalyzed glucose oxidation, to be enriched around the MNPs and copper crystals, leading to the establishment of a substrate channeling environment, resulting in the significantly enhanced cascade enzyme activity required for glucose detection.[40]

We then applied MNPs-GOx NFs for one-step glucose detection. From analysis of dose-response curves, the limit of detection (LOD) for glucose was determined to be as low as 2.5×10^{-6} M with a linear range of 5×10^{-6}–150×10^{-6} M (Figure 5c). Although the previous reports using GOx/HRP bienzyme system showed a lower detection limit down to 0.3×10^{-6} M, the LOD and linear range values of our system are comparable to the best of recent reports describing nanostructures-based measurements of glucose (Table S2, Supporting

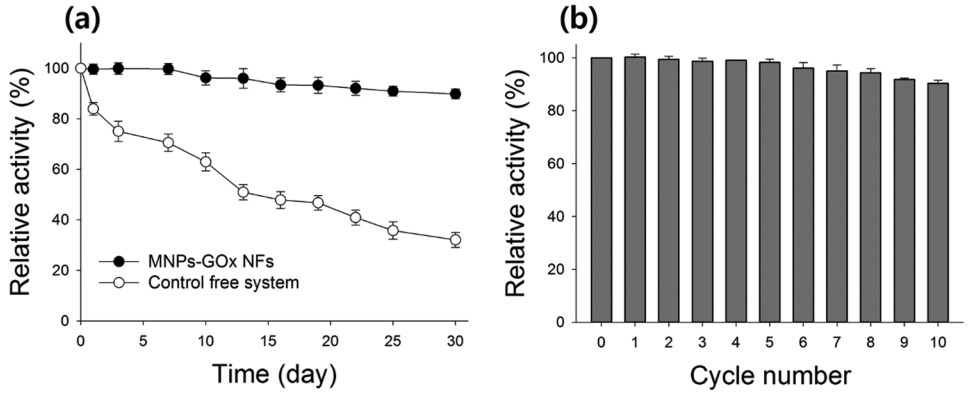

Figure 6. a) Long-term operational stability and b) magnetic reusability of the MNPs-GOx NFs for glucose detection.

Information).[41,42] The proposed system also shows excellent selectivity toward the corresponding target glucose, while no significant fluorescence was generated by negative control sugars such as lactose, sucrose, maltose, arabinose, and fructose, even at tenfold higher concentrations (Figure 5d). Selectivity of MNPs-GOx NFs was further investigated by examining the effects of the potentially interfering substances including ascorbic acid, amino acids, glutathione, human serum albumin, and metal ions, commonly present in human blood, on the detection of glucose. As a result, there was no significant signal of the employed substances (Figure S7, Supporting Information). These results demonstrate that a sensitive and selective reaction toward only the target glucose is promoted by the MNPs-GOx NFs.

Another advantage of the MNPs-GOx NFs based biosensor is its enhanced operational stability. During ≈1 month incubation at RT under nonshaking conditions, no significant decrease in activity was observed with MNPs-GOx NFs, whereas the control system composed of free MNPs, free GOx, and BSA NFs displayed a significant loss of activities (below 40%) (**Figure 6**a), probably due to the natural instability of free GOx. MNPs-GOx NFs were also proven to be stable over a broad range of pH from 2 to 10, whereas the control system lost almost half of its activity at low and high pH's, demonstrating their practical applicability (Figure S8, Supporting Information). The new glucose biosensing system is also expected to be easily separated from the solution by applying an external magnetic force, due to the presence of MNPs within the nanoflowers. As a result, MNPs-GOx NFs were reusable, retaining over 90% of their initial activity after ten iterative cycles (Figure 6b). Such enhanced stability and magnetic reusability may rank MNPs-GOx NFs as effective and versatile for diverse applications.

Finally, the real diagnostic capability of this system was demonstrated by determining the glucose levels using human serum samples that contained representative levels of glucose corresponding to normal, boundary, and high stages of hyperglycemia (normal; ≤ 5.6×10^{-3} M, boundary; 5.6×10^{-3}–7×10^{-3} M, and high; >7×10^{-3} M).[43] Serum glucose levels higher than 7×10^{-3} M when fasting are generally recognized to be indicative of high stage hyperglycemia, which can cause damage to internal organs in human.[43] To avoid and properly deal with hyperglycemia, particularly for people with diabetes, minimizing long-term exposure to high blood sugar levels by efficient testing them is essentially needed. The original amount of glucose in the serum sample was first determined using a glucose assay kit (Sigma-Aldrich, USA) and then a predetermined amount of glucose was further added to make the representative levels. As a result, serum glucose levels were quantified with excellent precision yielding CVs in the range of 4.4–6.2% and recovery rates of 100.9–103.9% (**Table 1**), thus verifying the excellent reproducibility and reliability of the current method. These observations demonstrate that the MNPs-GOx NFs based assay system can serve as a promising analytical tool to diagnose high glucose levels in clinical settings.

3. Conclusions

We have demonstrated the development of nanoparticle-incorporated enzyme nanoflowers, which allows for the close proximity of inorganic MNPs and GOx within copper-based nanoflowers. The MNPs-GOx NFs have highly enhanced peroxidase activity as well as substrate channeling for cascade reaction, leading to a highly specific and sensitive glucose detection system, along with excellent operational stability and magnetic reusability. The analytical utility of this new biosensor was demonstrated by its use in diagnosing high level of glucose in human blood serum. The simple protocol for the synthesis of

Table 1. Detection precision of the MNPs-GOx NFs-based assay system for the determination of glucose levels in spiked human serum samples.

	Original amount [× 10^{-3} M]	Added [× 10^{-3} M]	Expected [× 10^{-3} M]	Measured[a] [× 10^{-3} M]	SD[b]	CV[c] [%]	Recovery[d] [%]
Normal	4.04	0	4.04	4.07	0.253	6.2	100.9
Boundary		2	6.04	6.28	0.357	5.7	103.9
High		6	10.04	10.19	0.450	4.4	101.5

[a]Mean of six independent measurements; [b]Standard deviation of six measurements; [c]Coefficient of variation; [d]Measured value/expected value × 100.

MNPs-GOx NFs has opened up a great potential, not only for the development of enzyme-inorganic hybrid nanoflowers with the substrate channeling mechanisms but also for application in rapid, robust, and convenient detection of clinically important target molecules.

4. Experimental Section

See detailed description of experimental materials and methods in the Supporting Information.

Supporting Information

Supporting Information is available from the Wiley Online Library or from the author.

Acknowledgements

This work was supported by the National Research Foundation of Korea (NRF) grant funded by the Korea government [Ministry of Science and ICT (NRF- 2017R1C1B2009460)]. This work was also supported by the Global Research Laboratory Program (2014K1A1A2043032) and Nano-Material Technology Development Program (2014M3A7B4052193) through the National Research Foundation of Korea (NRF) grants funded by the Korea government Ministry of Science and ICT.

Conflict of Interest

The authors declare no conflict of interest.

Keywords

enzyme-inorganic hybrid nanoflowers, glucose detection, magnetic nanoparticles, peroxidase-like activity, substrate channeling

Received: November 22, 2018
Revised: February 5, 2019
Published online:

[1] M. Rahman, A. J. S. Ahammad, J. H. Jin, S. J. Ahn, J. J. Lee, *Sensors* **2010**, *10*, 4855.
[2] H. Lee, Y. J. Hong, S. Baik, T. Hyeon, D. H. Kim, *Adv. Healthcare Mater.* **2018**, *7*, 1701150.
[3] D. M. Nathan, D. E. R. Group, *Diabetes Care* **2014**, *37*, 9.
[4] S. W. Lee, S. A. Cheon, M. I. Kim, T. J. Park, *J. Nanobiotechnol.* **2015**, *13*, 54.
[5] Z. X. Lei, C. L. Gao, L. Chen, Y. T. He, W. D. Ma, Z. A. Lin, *J. Mater. Chem. B* **2018**, *6*, 1581.
[6] J. Ge, J. D. Lei, R. N. Zare, *Nat. Nanotechnol.* **2012**, *7*, 428.
[7] K. S. Park, B. S. Batule, M. Chung, K. S. Kang, T. J. Park, M. I. Kim, H. G. Park, *J. Mater. Chem. B* **2017**, *5*, 2231.
[8] B. S. Batule, K. S. Park, M. I. Kim, H. G. Park, *Int. J. Nanomed.* **2015**, *10*, 137.
[9] Y. X. Li, G. M. Xie, J. H. Qiu, D. D. Zhou, D. Gou, Y. Y. Tao, Y. Li, H. Chen, *Sens. Actuators, B* **2018**, *258*, 803.
[10] Z. Lin, Y. Xiao, Y. Q. Yin, W. L. Hu, W. Liu, H. H. Yang, *ACS Appl. Mater. Interfaces* **2014**, *6*, 10775.
[11] Z. Lin, Y. Xiao, L. Wang, Y. Q. Yin, J. N. Zheng, H. H. Yang, G. N. Chen, *RSC Adv.* **2014**, *4*, 13888.
[12] H. Li, J. W. Hou, L. L. Duan, C. Ji, Y. T. Zhang, V. Chen, *J. Hazard. Mater.* **2017**, *338*, 93.
[13] M. Chung, T. L. Nguyen, T. Q. N. Tran, H. H. Yoon, I. T. Kim, M. I. Kim, *Appl. Surf. Sci.* **2018**, *429*, 203.
[14] M. Chung, Y. J. Jang, M. I. Kim, *J. Nanosci. Nanotechnol.* **2018**, *18*, 6555.
[15] Z. X. Li, Y. F. Zhang, Y. C. Su, P. K. Ouyang, J. Ge, Z. Liu, *Chem. Commun.* **2014**, *50*, 12465.
[16] J. Y. Sun, J. C. Ge, W. M. Liu, M. H. Lan, H. Y. Zhang, P. F. Wang, Y. M. Wang, Z. W. Niu, *Nanoscale* **2014**, *6*, 255.
[17] T. X. Wei, D. Du, M. J. Zhu, Y. H. Lin, Z. H. Dai, *ACS Appl. Mater. Interfaces* **2016**, *8*, 6329.
[18] Y. C. Liu, J. Y. Chen, M. Y. Du, X. X. Wang, X. H. Ji, Z. K. He, *Biosens. Bioelectron.* **2017**, *92*, 68.
[19] R. F. Ye, C. Z. Zhu, Y. Song, Q. Lu, X. X. Ge, X. Yang, M. J. Zhu, D. Du, H. Li, Y. H. Lin, *Small* **2016**, *12*, 3094.
[20] R. F. Ye, C. Z. Zhu, Y. Song, J. H. Song, S. F. Fu, Q. Lu, X. Yang, M. J. Zhu, D. Du, H. Li, Y. H. Lin, *Nanoscale* **2016**, *8*, 18980.
[21] I. L. Medintz, H. T. Uyeda, E. R. Goldman, H. Mattoussi, *Nat. Mater.* **2005**, *4*, 435.
[22] D. J. Milliron, S. M. Hughes, Y. Cui, L. Manna, J. B. Li, L. W. Wang, A. P. Alivisatos, *Nature* **2004**, *430*, 190.
[23] I. J. M. de Vries, W. J. Lesterhuis, J. O. Barentsz, P. Verdijk, J. H. van Krieken, O. C. Boerman, W. J. G. Oyen, J. J. Bonenkamp, J. B. Boezeman, G. J. Adema, J. W. M. Bulte, T. W. J. Scheenen, C. J. A. Punt, A. Heerschap, C. G. Figdor, *Nat. Biotechnol.* **2005**, *23*, 1407.
[24] J. Y. Lee, C. Crake, B. Teo, D. Carugo, M. de Saint Victor, A. Seth, E. Stride, *Adv. Healthcare Mater.* **2017**, *6*, 1601246.
[25] L. M. Rossi, N. J. S. Costa, F. P. Silva, R. Wojcieszak, *Green Chem.* **2014**, *16*, 2906.
[26] L. Z. Gao, J. Zhuang, L. Nie, J. B. Zhang, Y. Zhang, N. Gu, T. H. Wang, J. Feng, D. L. Yang, S. Perrett, X. Yan, *Nat. Nanotechnol.* **2007**, *2*, 577.
[27] M. F. Li, M. Y. Luo, F. Li, W. W. Wang, K. Liu, Q. Z. Liu, Y. D. Wang, Z. T. Lu, D. Wang, *J. Phys. Chem. C* **2016**, *120*, 17348.
[28] Y. Y. Huang, X. Ran, Y. H. Lin, J. S. Ren, X. G. Qu, *Chem. Commun.* **2015**, *51*, 4386.
[29] Z. F. Wu, Z. Wang, Y. Zhang, Y. L. Ma, C. Y. He, H. Li, L. Chen, Q. S. Huo, L. Wang, Z. Q. Li, *Sci. Rep.* **2016**, *6*, 22412.
[30] N. Balistreri, D. Gaboriau, C. Jolivalt, F. Launay, *J. Mol. Catal. B: Enzym.* **2016**, *127*, 26.
[31] R. Wilson, A. P. F. Turner, *Biosens. Bioelectron.* **1992**, *7*, 165.
[32] R. A. Bini, R. F. C. Marques, F. J. Santos, J. A. Chaker, M. Jafelicci, *J. Magn. Magn. Mater.* **2012**, *324*, 534.
[33] Y. Yu, X. Fei, J. Tian, L. Q. Xu, X. Y. Wang, Y. Wang, *Colloids Surf., B* **2015**, *130*, 299.
[34] H. R. Lee, M. Chung, M. I. Kim, S. H. Ha, *Enzyme Microb. Technol.* **2017**, *105*, 24.
[35] V. A. J. Silva, P. L. Andrade, M. P. C. Silva, A. Bustamante, L. D. Valladares, J. A. Aguiar, *J. Magn. Magn. Mater.* **2013**, *343*, 138.
[36] J. P. Ge, Y. X. Hu, M. Biasini, W. P. Beyermann, Y. D. Yin, *Angew. Chem., Int. Ed.* **2007**, *46*, 4342.
[37] M. I. Kim, J. Shim, T. Li, J. Lee, H. G. Park, *Chem. - Eur. J.* **2011**, *17*, 10700.
[38] H. Y. Shin, B. G. Kim, S. Cho, J. Lee, H. B. Na, M. I. Kim, *Microchim. Acta* **2017**, *184*, 2115.
[39] F. Q. Yu, Y. Z. Huang, A. J. Cole, V. C. Yang, *Biomaterials* **2009**, *30*, 4716.
[40] M. Mathesh, J. Q. Liu, C. J. Barrow, W. R. Yang, *Chem. - Eur. J.* **2017**, *23*, 304.
[41] Q. Y. Liu, H. Li, Q. R. Zhao, R. R. Zhu, Y. T. Yang, Q. Y. Jia, B. Bian, L. H. Zhuo, *Mater. Sci. Eng., C* **2014**, *41*, 142.
[42] Y. L. Liu, X. J. Zhao, X. X. Yang, Y. F. Li, *Analyst* **2013**, *138*, 4526.
[43] D. R. Nair, M. Sharifi, K. Al-Rasadi, *Curr. Opin. Cardiol.* **2014**, *29*, 381.